Wave Vector Dependent Light Scattering Intensities by Polar Modes in GaAs

M. Nippus and R. Claus

Sektion Physik der LM-Universität München, Schellingstr. 4, 8000 München 40, FRG

(Z. Naturforsch. **32 a**, 731–735 [1977]; received June 2, 1977)

Light scattering intensities by the polaritons of F_2-type in GaAs have been experimentally studied. The spectra were excited by an YAG: Nd^{3+} laser in the infrared. When using the scattering intensities derived from the polar TO- and LO-phonons as input data for calculations, the k-dependent intensities in the polariton region could be verified within less than a few percent. The intensity variation for larger wave vectors was more precisely to be determined and verified than the frequency shifts.

Introduction

The semiconductor GaAs belongs to the space group T_d^2 ($= F\bar{4}3\,m$). The cubic unit cell contains four formula units. The primitive cell, however, contains only one, and consequently, factor group analysis predicts three optical branches: $\Gamma(T_d) = F_2$ which are simultaneously Raman- and infrared-active. Because of electrostatic interaction the transverse-longitudinal mode degeneracy is lifted. The optical phonons for $k \approx 10^5\,\mathrm{cm}^{-1}$ are F_2(TO) at 268 cm^{-1} and F_2 (LO) at 292 cm^{-1}. The band gap in GaAs with ~ 1.4 eV is relatively small. The lowest exciton absorption edge is to be found at $\sim 1\,\mu$m and the highest frequency Reststrahlenband at $\sim 30\,\mu$m. Experiments show that also extremely pure samples always have some absorption within this region [1]. Light scattering therefore is performed most advantageously with laser sources in the infrared. The present studies were carried out by using a YAG: Nd^{3+}-laser with an exciting line $\lambda = 1.064\,\mu$m. In 1969 Patel and Slusher studied polariton dispersion in GaAs with different free carrier concentrations by the same type of laser. These experiments were the first to show the existence of real "plasmaritons" [2]. However, no attention was paid to the scattering intensities. Our present experiments show that the data which can be derived from scattering intensities in the polariton region are at least as informative as those concerning the energies. Polariton intensity measurements promise to become an important tool for light scattering studies on semiconductors.

Reprint requests to Dr. R. Claus, Sektion Physik der Universität München, Schellingstr. 4/III, *D-8000 München 40.*

Experimental

The output power of our YAG: Nd^{3+}-laser was ≈ 25 W. Because of different optical elements used and the high refractive index of GaAs the beam power inside the sample was reduced to ~ 4 W. The crystal sample was cubic (5.5 mm)^3 cut with edges along the [110]-, [1$\bar{1}$0]-, and [001]-directions, see Figure 1. Refractive indices were $n_i = 3.477$ and $n_s = 3.465$ for the incident and scattered radiation, respectively. The latter index holds for the Stokes-shifted TO-phonon at 268 cm^{-1}. The experimental set up used for observation of polaritons has been described in detail [3]. The laser beam was alternatively focused into the sample by two lenses: L_1 with $f = 30$ cm and 4 cm diameter, and L_2 with $f =$ 50 cm and 17 cm diameter. L_1 allowed a precise determination of the internal scattering angle φ and consequently the wave vector k for very near forward scattering from

$$k^2 = (2\pi n_i \nu_i)^2 + (2\pi n_s \nu_s)^2 - 8\pi n_i n_s \nu_i \nu_s \cos\varphi\,, \qquad (1)$$

see [4]. ν_i and ν_s herein are the vacuum wave numbers of the incident and scattered photons, respectively. The polariton spectra reproduced in Fig. 2 are recorded with this lens. L_2, on the other hand allowed the observation of polaritons with larger wave vectors and frequencies close to the TO-phonon. The highest frequency polariton observed was located at $\approx 262\,\mathrm{cm}^{-1}$. Internal scattering angles and wave vectors were less precisely to be determined. The intensity data derived from these experiments, however, still were informative and have been included as data points in Figure 3. We therefore present more experimental data points in the $|\chi(\nu)|$-diagram than in the $\nu(k)$-diagram. When regarding n_s as constant within the observable polariton region mode observation in principle should be possible towards $\nu = 0$ for $\varphi = 0$. Experiments show that this

does not happen, see Figure 2. We therefore extrapolated n_s by a linear approximation as

$$n(\omega_s) \approx n(\omega_i) - (\partial n/\partial\omega)_{\omega_i} |\omega_i - \omega_s| ,$$

see e. g. [4], p. 66, and References [5, 6]. The lowest frequency polariton recorded for $\varphi = 0$ then turns out to be expected only at $\nu \approx 210\,\mathrm{cm}^{-1}$ which is in good agreement with our experiments.

Results and Discussion

Raman scattering intensities generally can be calculated by the well known relation [7]:

$$I(\omega) = A \cdot \frac{(\omega_i \pm \omega)^4}{\omega} n(T, \omega) \cdot |\boldsymbol{e}_i \chi(\omega) \boldsymbol{e}_s|^2 . \quad (1)$$

Herein $\boldsymbol{e}_{i,s}$ are unit vectors describing the polarization of the incident and scattered photons, $n(T, \omega) = [\pm 1 \mp \exp(\mp \hbar\omega/kT)]^{-1}$ is the Bose-Einstein-factor, and A a constant containing information on the specific experiment (scattering volume etc). For light scattering by phonons with larger wave vectors ($k \approx 10^5\,\mathrm{cm}^{-1}$) in solids the susceptibility tensor $\chi(\omega)$ contains only higher order terms depending on internal macroscopic electric fields. Only in the polariton region also a linear term becomes of importance

$$\chi(\omega) = a\,\mathbf{Q}(\omega) + b\,\boldsymbol{E}(\omega) . \quad (2)$$

Tensors a and b have become known as the "atomic displacement"- and "electronic part of the electro-optic"-tensor. Their symmetries can be seen from tables, [4]. The normal coordinate $\mathbf{Q}(\omega)$ and the macroscopic field $\boldsymbol{E}(\omega)$ are related to one another by Huang's first equation

$$(\omega_T^2 - \omega^2)\,\mathbf{Q}(\omega) = B^{12}\,\boldsymbol{E}(\omega) , \quad (3)$$

where $B^{12} = \omega_T \sqrt{(\varepsilon_0 - \varepsilon_\infty)/4\pi}$, [4]. The choice of a suitable value for the high frequency dielectric constant ε_∞ is questionable in a material with a small band gap as GaAs, see [8]. We shall show, however, that ε_∞ not necessarily has to be known explicitely for calculations of polariton scattering intensities in diatomic cubic crystals when the LO-phonon intensities are used as input data. From (2) and (3) follows

$$\chi(\omega) = \left(\frac{a\,B^{12}}{\omega_T^2 - \omega^2} + b\right) \boldsymbol{E}(\omega) . \quad (4)$$

No normal coordinate appears explicitely in this equation. For a cubic diatomic crystal the mode strength is given by $S = \varepsilon_0 - \varepsilon_\infty$. S thus is related to B^{12} and the LO- and TO-phonon frequencies by

$$S = (\omega_L^2/\omega_T^2 - 1)\,\varepsilon_\infty = (4\pi/\omega_T^2)\,(B^{12})^2 . \quad (5)$$

For phonons with $k \approx 10^5\,\mathrm{cm}^{-1}$ the electric field $\boldsymbol{E}(\omega_T)$ vanishes. Equation (2) then leads to $|\chi(\omega_T)| = a$. $\boldsymbol{E}(\omega)$ in Eq. (4) therefore has to be determined so as to provide the same result for $\omega \to \omega_T$. Following a procedure proposed by Burstein et al.[9] and somewhat modified by the authors [3, 10] it follows

$$\boldsymbol{E}(\omega) = \left(\frac{\varepsilon_\infty}{4\pi} + \frac{\omega_T^2 (B^{12})^2}{(\omega_T^2 - \omega^2)^2}\right)^{-1/2} \omega\, E_0 . \quad (6)$$

E_0 is a normalization constant which may be set $= 1$ for calculations of relative intensities. Using (6) while taking into account (5) the susceptibility tensor (4) becomes

$$\chi(\omega) = \frac{[a\sqrt{\omega_L^2 - \omega_T^2} + \sqrt{4\pi/\varepsilon_\infty}\, b\,(\omega_T^2 - \omega^2)]\,\omega}{\sqrt{(\omega_T^2 - \omega^2)^2 + (\omega_L^2 - \omega_T^2)\,\omega_T^2}} . \quad (7)$$

For $\omega \to 0$ the susceptibility tensor vanishes. For $\omega \to \omega_L$ on the other hand, $\chi(\omega_L)$ inserted into (1) allows calculation of the LO-mode scattering intensity $I(\omega_L)$. This is easily realized too when considering that for $k = 0$ all transverse polariton branches expect for the lowest one end up at the frequencies of the longitudinal modes. The vibrational states degenerate. TO- and LO-modes are indistinguishable. Their macroscopic electric fields are identical $\boldsymbol{E} = -4\pi\boldsymbol{P}$, see [4], page 46. From (7) follows for $\omega \to \omega_L$

$$b = [a \pm |\chi(\omega_L)|] \sqrt{\frac{\varepsilon_\infty}{4\pi\,(\omega_L^2 - \omega_T^2)}} . \quad (8)$$

The uncertainty of a sign in this formula remains because the experiment provides only the magnitude of χ, see Equation (1). When combining (8) with (7) we finally obtain the frequency dependent susceptibility tensor for polaritons in diatomic cubic crystals in a form which seems best suited to experiments

$$|\chi(\omega)| = \frac{[a\sqrt{\omega_L^2 - \omega_T^2} + (a \pm |\chi(\omega_L)|)\,(\omega_T^2 - \omega^2)/\sqrt{\omega_L^2 - \omega_T^2}]\,\omega}{\sqrt{(\omega_T^2 - \omega^2)^2 + (\omega_L^2 - \omega_T^2)\,\omega_T^2}} . \quad (9)$$

The correct sign of $\pm|\chi(\omega_L)|$ is easily determined in each special case by checking the qualitative variation of the polariton intensities for $k \to 0$. We especially note that the uncertain quantity ε_∞ does not appear explicitely in this relation. This can be arranged to be only in simple diatomic crystals but not in more complicated materials. We believe, however, that it is of great importance for many III – V-compound semiconductors where a small bandgap never would allow a direct determination of ε_∞ with sufficient high accuracy as to prevent the possibility of experimental data fittings within rather broad limits, see [8]. We have in [8] shown that the problem cited is nontrivial also in insulators like $LiNbO_3$ with a much larger band gap.

In order to calculate the k-dependent scattering intensities from (1) and (9) it is most convenient to use $|\chi(\omega_L)|$ or the intensity ratio $I(\omega_L)/I(\omega_T)$ as experimental input data. This procedure eliminates all difficulties otherwise occurring with the atomic displacement tensor $a = \partial\chi/\partial Q$, i. e. the classical problems with spontaneous Raman scattering intensities. We shall show below that the remaining influence of the electrooptic term [second term in Eq. (2)] is covered with a surprising high accuracy by (9). The Raman tensor for polar F_2-modes in the factor group T_d can be written

$$R = \left\{ \begin{pmatrix} \cdot & \cdot & \cdot \\ \cdot & \cdot & f \\ \cdot & f & \cdot \end{pmatrix}, \begin{pmatrix} \cdot & \cdot & f \\ \cdot & \cdot & \cdot \\ f & \cdot & \cdot \end{pmatrix}, \begin{pmatrix} \cdot & f & \cdot \\ f & \cdot & \cdot \\ \cdot & \cdot & \cdot \end{pmatrix} \right\} \qquad (10)$$

a and b can be combined to one tensor of type (10). This is generally possible only in diatomic crystals, see [4], Appendix 4. χ in Eq. (1) therefore can be written in condensed form as

$$f \begin{pmatrix} 0 & a u_z + \beta v_z & a u_y + \beta v_y \\ a u_z + \beta v_z & 0 & a u_x + \beta v_x \\ a u_y \beta v_y & a u_x + \beta v_x & 0 \end{pmatrix} \qquad (11)$$

$u_{x,y,z}$ and $v_{x,y,z}$ are the components of unit vectors, respectively, of the mechanical displacement and the electric field for the principal directions. α and β correspond to a and b in Equation (8). When measuring only relative scattering intensities f can be included in the constant A. For transverse phonons with $k \approx 10^5\ \mathrm{cm}^{-1}$ recorded e. g. by right angle geometries $\beta \equiv 0$. The orientation of the sample was already described and has been sketched in Figure 1. The 4 combinations of e_i and e_s parallel ($\parallel$) and perpendicular ($\perp$) to the scattering plane S indicated in Fig. 1 provide Raman intensities proportional to $|\chi(\omega_T)|^2$ and $|\chi(\omega_L)|^2$ as summarized in Table 1. Corresponding Raman spectra are shown in Figure 1. Except for slight deviations ($\lesssim \pm 6\%$) due to the apparatus the observed data are in good agreement with the calculated coefficients in Table 1. The average of the ratio of the integrated intensities

Table 1. Raman scattering intensities $I \sim |\chi(\omega_T)|^2$ and $I \sim |\chi(\omega_L)|^2$ corresponding to the four combinations of e_i and e_s when using the right angle scattering geometries sketched in Figure 1.

e_i	e_s	$\nu_T = 268\ \mathrm{cm}^{-1}$ $\lvert\chi(\omega_T)\rvert^2$	$\nu_L = 292\ \mathrm{cm}^{-1}$ $\lvert\chi(\omega_L)\rvert^2$
$\parallel$	$\parallel$	$\frac{2}{3}\alpha^2$	$\frac{2}{3}(\alpha+\beta)^2$
$\perp$	$\parallel$	α^2	0
$\parallel$	$\perp$	0	0
$\perp$	$\perp$	$\frac{1}{3}\alpha^2$	$\frac{1}{3}(\alpha+\beta)^2$

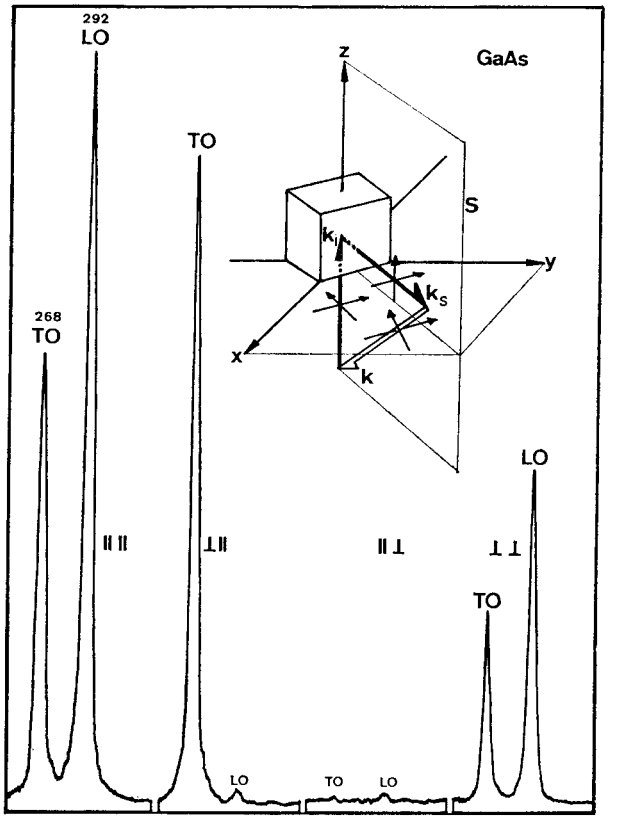

Fig. 1. First order phonon spectra of GaAs at 300 K. The scattering geometries used can be seen from the inserted figure and the text. Laser: YAG:Nd^{3+} at 1.064 μm, output 1 W, spectral slit width 3 cm^{-1}, maximum counts 500 cps, period = 1 s, cooled S–1 multiplier (–90 °C).

derived from 10 spectra recorded with ($\|\,\|$)- and ($\perp\,\perp$)-geometries provides $I(\omega_L)/I(\omega_T) = 1.74 \pm 6\%$. When defining $|\chi(\omega_T)| = a = 1$ and taking into account the ω^4-law and a sample temperature of ≈ 300 K it follows $|\chi(\omega_L)| = 1.41 \pm 0.04$. Earlier measurements lead to $I(\omega_L)/I(\omega_T) = 1.53 \pm 20\%$, see [11]. The half widths derived from our experiments were $2\Gamma_T = 4.5 \pm 0.2$ and $2\Gamma_L = 4.1 \pm 0.1$ cm^{-1}. The spectral slit width used was 2.7 cm^{-1}. Our data agree with those reported by Mooradian [12] whereas those reported by Ref. [11] are remarcably smaller. The signs of the atomic displacement- and electrooptic-tensor elements were determined to be sign $a = -1$ and sign $b = +1$. By using these input data $|\chi(\nu)|$ has been calculated and plotted in the upper diagram of Fig. 3 (curve A). At ≈ 192 cm^{-1} the polariton scattering intensity is expected to vanish. This is due to the well known effect that the electrooptic and atomic displacement contributions to χ may cancel when a and b have opposite signs, see (2). Figure 2 shows a spectra series beautifully demonstrating the recorded intensity variation. The TO-phonon appears due to some backscattering. In order to calculate $\chi(\nu)$ numerically from these spectra the constant factor in Eq. (1) was set $= 1$. The agreement found between theory and experiment was surprisingly good. When comparing the $|\chi(\nu)|$-diagram with the polariton dispersion curve $\nu = \nu(k)$ which has been reproduced in the lower diagram of Fig. 3 one finds that the sensitivity of the intensity experiments as a matter of fact exceeds that of the frequency dispersion measurements in the region where the $\nu(k)$-branch still is relatively flat. This shows clearly that polariton scattering intensities should not be overlooked as a source of information especially in some III – V-compound semiconductors.

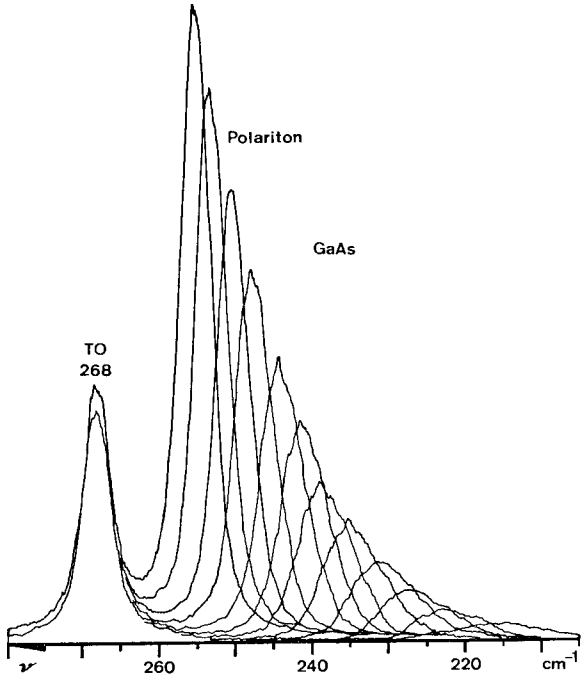

Fig. 2. Polariton spectra of GaAs at 300 K. Laser output 4 W, spectral slit width 2.7 cm^{-1}, maximum counts 500 cps, period = 4 s, cooled S–1 multiplier at −90 °C. The TO-phonon at 268 cm^{-1} appears due to some backscattering.

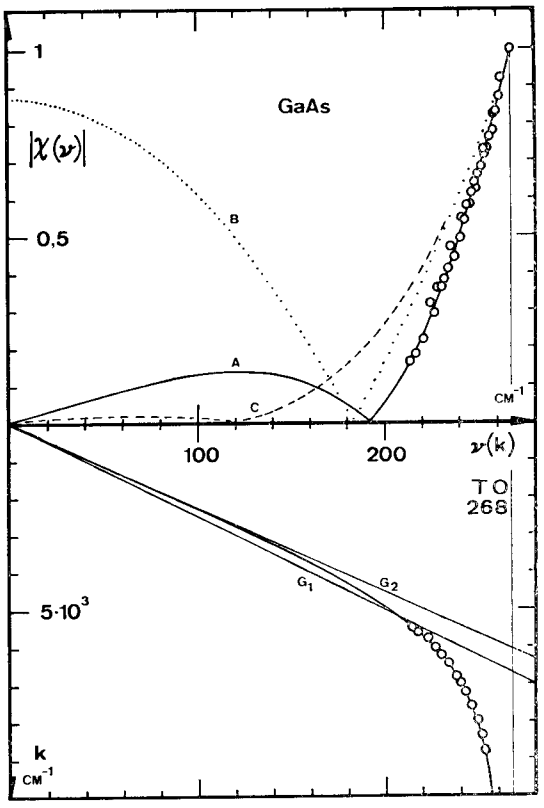

Fig. 3. Upper diagram: calculated susceptibility tensor for GaAs, curve A, and experimental data. Curves B and C were calculated on the basis of other authors data and formulas, see text. Lower-diagram: polariton dispersion curve $\nu(k)$ plotted so that a direct comparison with curve A in the upper diagram is made possible. G_1 and G_2 are "limiting lines" for observation, see [4] calculated with $(\partial n/\partial \nu)_{\nu_i} = 4.64 \cdot 10^{-5}$ cm, and without dispersion taken into account, see text.

Damping coefficients do not appear explicitely in our above calculations by essentially two reasons. a) $\Gamma(\omega)$ turns out to be almost constant in the observable polariton region, see Figure 2. Integrated

intensities therefore are directly proportional to peak intensities which are provided by Equations (1) and (9). When comparing these equations with the equivalent relation (3.69) in [15] a Lorentz-factor seems to be lost. The influence of this Lorentzian, however, is included in our procedure of evaluating the spectra. We determined integrated intensities and not the differential intensity as a function of ω as provided by (3.69) in [15]. b) Strictly Huang's first Eq. (3) above should also include a damping term. The following calculations are easily rearranged in this way. $|\chi(\omega)|$ in (9) then has to be determined as the magnitude of the complex function. Our experiments, however, show that susceptibilities calculated in this way differ only within the experimental error from those derived from (9). This turns out to be true in GaAs. It has of course to be checked carefully in other materials before applying Eq. (9) in the form given above.

The diverging experimental phonon intensity data reported in Ref. [11] do not predict polariton intensities which are in satisfying agreement with our measurements, dashed curve C in Figure 3. We also want to point out that some authors in the past have used formulas to calculate polariton scattering intensities which contain too rough approximations as to provide reliable results. Our above treatment is equivalent to that given earlier by Loudon [14] and Barker and Loudon [15], see Eq. (3.69) therein. Polariton intensities in zinc blende have been calculated in Ref. [13] while essentially neglecting the $\boldsymbol{E}(\omega)$-dependence given above by Equation (6). Equations $(2-2)$ and $(2-3)$ in [13] do not contain the ω-dependence included in the denominators of Eq. (43) in [14], Eq. (3.69) in [15], or (9) above. The dotted curve B in Fig. 3 shows the result obtained from Eqs. $(2-2)$ and $(2-3)$ in [13]. We have avoided explicitely to use ε_∞ ($\equiv \varepsilon_0$ in Ref. [13]) in the same way as described in our treatment above. The curve obviously differs also qualitatively from the others! Calculations of the "electrooptic and deformation potential contributions to the Raman tensor in CdS" [16] have been carried out on the basis of a similarly approximated formula: (1) in [16]. The ω-dependence which should appear in the denominator again is lost.

Acknowledgement

We thank Prof. J. Brandmüller for his interest in this work. We are furthermore grateful to Messerschmitt-Bölkow-Blohm for providing the laser, the Brauns-Heitmann KG, Chem. Betriebe, Bad Abling for providing a computer, and the Bayerische Staatsoper for supporting us with the big lens L_2.

[1] M. G. Milvidskii, V. B. Osvenskii, E. P. Rashevskaya, and T. G. Yngova, Sov. Phys. Sol. State **7**, 2784 [1966].
[2] C. K. N. Patel, and R. E. Slusher, Phys. Rev. Lett. **22**, 282 [1969].
[3] M. Nippus, Thesis, Munich 1977.
[4] R. Claus, L. Merten, and J. Brandmüller, Springer Tracts in Modern Physics **75** [1975].
[5] D. T. F. Marple, J. Appl. Phys. **35**, 1241 [1964].
[6] B. O. Seraphin and H. E. Benett, in Semicond. and Semimet, Vol. 3, ed. R. K. Willardson and A. C. Beer, Acad. Press Inc. N. Y. 1967.
[7] G. Placzek, Rayleigh-Streuung und Raman-Effekt in Handbuch der Radiologie, Bd. VI—II, Leipzig 1934.
[8] E. Schuller, R. Claus, and H. J. Falge, Z. Naturforsch. **32a**, 47 [1977].
[9] E. Burstein, S. Ushioda, and A. Pinczuk, in Light Scattering Spectra of Solids, Springer-Verlag, New York 1969, p. 43.
[10] M. Nippus and R. Claus, Z. Naturforsch. to be published.
[11] W. D. Johnston and I. P. Kaminov, Phys. Rev. **188**, 1209 [1969].
[12] A. Mooradian, Lincoln, Lab. Rep. S-9331, MIT, Lexington, Mass. [1970].
[13] S. Ushioda, A. Pinczuk, E. Burstein, and D. L. Mills, in Light Scattering Spectra, Solids, Springer-Verlag, New York 1969, p. 347.
[14] R. Loudon, in Light Scattering Spectra of Solids, Springer-Verlag, New York 1969, p. 25.
[15] A. S. Barker and R. Loudon, Rev. Mod. Phys. **44**, 18 [1972].
[16] J. F. Scott, T. C. Damen, and J. Shah, Opt. Commun. **3**, 384 [1971].